AGU PUBLICATIONS

JGR

Journal of Geophysical Research: Atmospheres

RESEARCH ARTICLE
10.1002/2014JD022364

Key Points:
- The spring VM significantly affects the ITCZ during the following summer
- The VM and ENSO may together act as effective predictors of ITCZ precipitation
- A VM-based model is a useful predictive tool for Pacific summer precipitation

Correspondence to:
J. Li,
ljp@bnu.edu.cn

Citation:
Ding, R., J. Li, Y.-h. Tseng, and C. Ruan (2015), Influence of the North Pacific Victoria mode on the Pacific ITCZ summer precipitation, *J. Geophys. Res. Atmos.*, *120*, 964–979, doi:10.1002/2014JD022364.

Received 27 JUL 2014
Accepted 2 JAN 2015
Accepted article online 8 JAN 2015
Published online 10 FEB 2015

Influence of the North Pacific Victoria mode on the Pacific ITCZ summer precipitation

Ruiqiang Ding[1], Jianping Li[2], Yu-heng Tseng[3], and Chengqing Ruan[1]

[1]State Key Laboratory of Numerical Modeling for Atmospheric Sciences and Geophysical Fluid Dynamics, Institute of Atmospheric Physics, Chinese Academy of Sciences, Beijing, China, [2]College of Global Change and Earth System Sciences, Beijing Normal University, Beijing, China, [3]Climate and Global Dynamics Division, NCAR, Boulder, Colorado, USA

Abstract This study demonstrates the close connection between the second dominant mode of spring sea surface temperature anomalies (SSTAs) in the North Pacific poleward of 20°N, referred to as the Victoria mode (VM), and the Pacific Intertropical Convergence Zone (ITCZ) precipitation during the following summer. Our analysis shows that strong positive VM cases are followed by positive precipitation anomalies over the central-eastern Pacific ITCZ region, in association with negative precipitation anomalies over the ITCZ regions of the tropical western Pacific and eastern North Pacific. The hypothesized physical mechanism through which the spring VM induces the Pacific ITCZ summer precipitation is similar to but slightly different from the seasonal footprinting mechanism. During strong positive VM cases, SSTAs in the subtropics associated with the spring VM persist until summer and develop toward the equator, where low-level convergence and divergence caused by SSTA gradients give rise to enhanced precipitation over the central-eastern Pacific ITCZ region and to reduced precipitation over the ITCZ regions of the tropical western Pacific and eastern North Pacific. The thermodynamic ocean-atmosphere coupling between the ITCZ and SSTAs associated with the VM may play a vital role in the initiation of El Niño–Southern Oscillation (ENSO) events. The VM influence on tropical Pacific summer precipitation can be passed on to the next year through its influence on ENSO. A VM-based linear model is established to predict the tropical Pacific summer precipitation, which yields skillful forecasts for summer precipitation across almost the entire tropical Pacific.

1. Introduction

The Intertropical Convergence Zone (ITCZ) is a belt of low pressure that circles the Earth near the equator, where the trade winds originating from the Northern and Southern Hemispheres converge. Convergence of interhemispheric trade winds leads to strong convection and heavy precipitation within the ITCZ. Air rises in the ITCZ, moves poleward in the upper troposphere, and sinks in the subtropics; i.e., the ITCZ constitutes the ascending branch of the Hadley cell. The nonuniform distribution of land and sea causes the shape of the ITCZ to vary with longitude. In the western Pacific, the ITCZ is broader in latitude, mainly owing to the large warm pool in the ocean, while in the eastern Pacific, the ITCZ is narrow and long, and generally located at the southern boundary of the eastern Pacific warm pool, north of the strongest meridional gradient of sea surface temperature (SST) [*Yin and Albrecht*, 2000; *Raymond et al.*, 2003].

The significant impact of local tropical influences on variations in the position and intensity of the ITCZ on interannual timescales has been widely recognized in previous studies [e.g., *Zheng et al.*, 1997; *Chiang et al.*, 2002; *Hastenrath*, 2002; *Gu et al.*, 2005; *Münnich and Neelin*, 2005; *Chou and Lo*, 2007; *Zhan et al.*, 2011]. In contrast, extratropical forcing is not typically considered one of the important factors driving the interannual variability of the ITCZ. However, much paleoclimatic and modeling evidence has been reported regarding extratropical influences on the ITCZ, including the effects of high-latitude land ice, sea ice, and ocean heat transport [*Chiang et al.*, 2003; *Chiang and Bitz*, 2005], the Atlantic thermohaline circulation [*Zhang and Delworth*, 2005], antisymmetric interhemispheric heating [*Broccoli et al.*, 2006], extratropical thermal forcing [*Kang et al.*, 2008, 2009], and so on. Changes in all of these extratropical forcing factors have been shown to cause distinct southward or northward shifts in the location of the ITCZ.

In recent years, the Victoria mode (VM), defined as the second empirical orthogonal function mode (EOF2) of SST anomalies (SSTAs) in the North Pacific poleward of 20°N [*Bond et al.*, 2003], has been introduced to describe aspects of North Pacific climate variability that cannot be explained by the Pacific Decadal Oscillation (PDO) [*Mantua et al.*, 1997; *Zhang et al.*, 1997] alone; the PDO is known as the EOF1 of SSTAs in the extratropical North

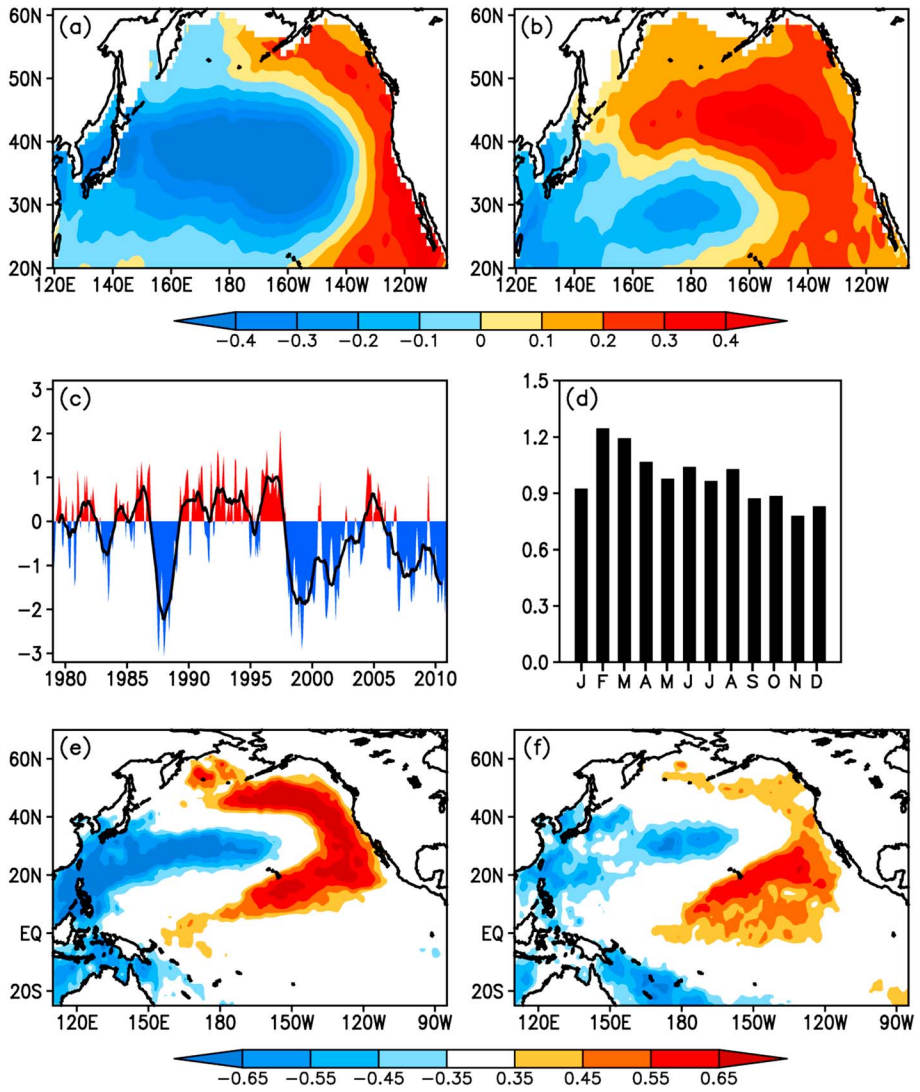

Figure 1. (a) Spatial patterns of the (a) EOF1 and (b) EOF2 modes of the North Pacific (120°E–100°W, 20–61°N) monthly SSTA field (after removing the monthly mean global average SSTAs). EOF1 and EOF2 account for 24.8% and 15.9% of the total variance, respectively. (c) The second principal component (PC2) time series associated with EOF2. Monthly values of PC2 time series are indicated by colored bars (red, positive; blue, negative) with a 13 month running mean overlain (bold lines). (d) Seasonal variations of the standard deviation of the VM index. (e) Correlation maps of the spring (FMA) VM index with the spring SSTAs. Positive (red) and negative (blue) SSTAs, with correlation significant at the 95% level, are shaded. (f) As for Figure 1e but for correlation maps of the spring VM index with the summer (MJJ) SSTAs.

Pacific (see Figure 1a for its spatial pattern). The VM exhibits a distinct northeast-southwest oriented SSTA dipole pattern, characterized by a band of positive SSTAs extending from off California across the Pacific to the western Bering Sea and a band of negative SSTAs extending from the central North Pacific to the coast of Asia [*Bond et al.*, 2003] (see also Figure 1b). The VM index (the second principal component (PC2) time series associated with the EOF2) shows marked interannual variability (Figure 1c). Previous studies have shown how the North Pacific Oscillation (NPO)-like atmospheric variability induces changes in surface heat fluxes, which subsequently generate a dipole SSTA pattern in the North Pacific poleward of 20°N [*Vimont et al.*, 2003a, 2003b; *Alexander et al.*, 2010; *Yu and Kim*, 2011]. Figure 1d illustrates that the VM attains maximum variance in spring (February–April (FMA)). By examining the spatial patterns of the spring and summer (May–July (MJJ)) averaged SSTAs correlated with the spring VM index, it is noticed that during spring when the VM peaks, the VM-related significant SSTAs are not just confined to the North Pacific poleward of 20°N (the domain over which the VM is defined) but extend into the tropics (Figure 1e). These SSTAs associated with

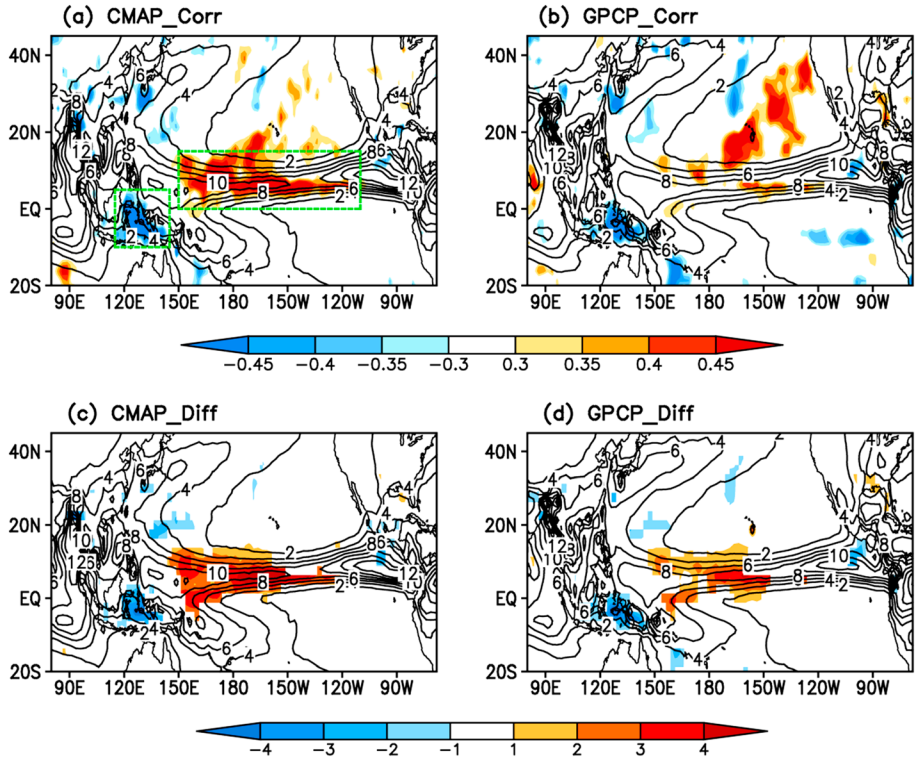

Figure 2. (a) Correlation maps of the spring (FMA) VM index with the Pacific summer (MJJ) precipitation anomalies based on the CMAP data set and (c) composite differences in tropical Pacific summer precipitation anomalies (mm d^{-1}) between strongly positive and negative VM cases (strongly positive minus negative VM cases). (b and d) As for Figures 2a and 2c, respectively, but based on the GPCP data set. In Figures 2a and 2b, areas with correlation coefficients significant at the 90% level are shaded. In Figures 2c and 2d, only precipitation anomalies significant at the 90% level are shown. In Figures 2a–2d, the climatological (1979–2010) summer mean precipitation is superposed as contours. In Figure 2a, the two green boxes are the positive correlation box (0°N–15°N, 150°E–110°W) and the negative correlation box (10°S–5°N, 115°E–145°E), which indicate the locations of the CI and WI regions, respectively.

the spring VM (mainly its related subtropical portion) can persist into the ensuing summer (Figure 1f), presumably affecting the tropical Pacific climate system during summer, such as on the Pacific ITCZ summer precipitation.

Motivated by the persistence of the VM-related SSTAs from spring to summer in Figure 1, this study aims to establish the delayed influence of the spring VM on the Pacific summer ITCZ. Since the ITCZ is such a critical element of both the tropical and global climate, a better understanding of how the VM influences the Pacific ITCZ should significantly improve climate predictions in the tropical Pacific and other regions. Nonetheless, the influence of the VM on the Pacific ITCZ has not been documented in the literature. Consequently, we believe that the significance of our study is twofold. First, it provides further observational evidence of the influence of extratropical forcing on the ITCZ based on the latest observational data. Second, the tropical mean climate is not well simulated by the current generation of coupled general circulation models [e.g., *Delecluse et al.*, 1998; *Davey et al.*, 2002; *Meehl et al.*, 2005; *Lin*, 2007], and our results suggest that a better simulation of the spring VM may help to improve the prediction of the Pacific ITCZ during summer.

2. Data and Methods

2.1. Observational Data

The basic precipitation data used in this study were the Climate Prediction Center Merged Analysis of Precipitation (CMAP) data set [*Xie and Arkin*, 1997]. Data from the Global Precipitation Climatology Project (GPCP) data set [*Huffman et al.*, 1997; *Adler et al.*, 2003] were also used to verify the CMAP results. The CMAP and GPCP data sets contain monthly precipitation data (mm d^{-1}) at a spatial resolution of 2.5° × 2.5°. The atmospheric circulation data used were the National Centers for Environmental Prediction–National Center

Table 1. Correlations Between the Spring VM Index, the Previous Winter's Niño3.4 Index, Area-Averaged Summer Precipitation Anomalies Over the CI and WI Regions Based on the CMAP Data Set, PC Time Series Associated With the First Two Dominant Modes of the Tropical Pacific Summer Precipitation Anomalies, and the Spring NPGO Index

	VM	Niño3.4	CI	WI	PC1	PC2	NPGO
VM	1						
Niño3.4	−0.03	1					
CI	0.59[b]	0.02	1				
WI	−0.53[a]	−0.28	−0.72[b]	1			
PC1	−0.05	0.67[b]	−0.03	−0.23	1		
PC2	0.55[a]	−0.04	0.93[b]	−0.86[b]	0.00	1	
NPGO	0.78[b]	0.24	0.46[a]	0.49[a]	0.17	0.45[a]	1

[a]Correlation significant at the 99% level.
[b]Correlation significant at the 99.9% level.

for Atmospheric Research (NCEP-NCAR) reanalysis on a 2.5°×2.5° grid [*Kalnay et al.*, 1996]. The SST data were the Hadley Center Sea Ice and SST data set (HadISST) on a 1°×1° spatial grid [*Rayner et al.*, 2006]. The Niño3.4 index is defined as the SST averaged over the region (170°W–120°W, 5°S–5°N). Monthly outgoing longwave radiation (OLR) data from the National Oceanic and Atmospheric Administration (NOAA) [*Liebmann and Smith*, 1996] were used to represent large-scale tropical convective activity over the tropical ocean and land. We analyzed the period 1979–2010, because the precipitation, NCEP-NCAR reanalysis, SST, and OLR data were all available for this time span.

2.2. Effective Number of Degrees of Freedom

We estimate the significance of all correlations between two time series taking into account the effect of their autocorrelations. For two time series of variables X and Y, the effective sample size N^* was estimated using the modified Chelton method [*Pyper and Peterman*, 1998; *Li et al.*, 2013]. The N^* can be obtained from the theoretical approximation

$$N^* \approx \frac{N}{1+2\sum_{i=1}^{N}\frac{N-i}{N}R_X(i)R_Y(i)}, \quad (1)$$

where N is the number of available time steps and $R_X(i)$ and $R_Y(i)$ are the autocorrelations of the two sampled time series $X(i)$ and $Y(i)$ (i=1,…,N), respectively.

3. Relationship Between the VM and ITCZ in the Pacific

To examine the possible connection between the spring VM and Pacific ITCZ summer precipitation, we show in Figure 2a the correlation between the FMA-averaged VM index and the MJJ-averaged precipitation anomalies from the tropical Pacific based on the CMAP data set. It is evident that the spring VM is strongly and positively correlated with summer precipitation anomalies over the central-eastern North Pacific ITCZ region (hereafter the CI region: 0°N–15°N, 150°E–110°W). In contrast, there are significant negative correlations between the spring VM and summer precipitation anomalies over the western Pacific ITCZ region around Indonesia (hereafter the WI region: 10°S–5°N, 115°E–145°E). We calculated the correlations between the spring VM index and area-averaged summer precipitation anomalies over the CI and WI regions (Table 1). The spring VM has a significant positive correlation with precipitation anomalies over the CI region (r = 0.59, significant at the 99.9% level), while it is also significantly correlated with precipitation anomalies over the WI region (r = −0.53, significant at the 99% level). In addition, there are weak negative correlations between the spring VM index and precipitation anomalies over the eastern North Pacific ITCZ region off the southwest coast of Mexico (hereafter the EI region).

To further investigate the link between the spring VM and Pacific ITCZ summer precipitation, we show the composite differences of the tropical Pacific summer precipitation anomalies between six strongly positive VM cases (1982, 1986, 1991, 1994, 1996, and 1997) and six strongly negative VM cases (1988, 1998, 1999, 2000, 2001, and 2008) (Figure 2c). These strongly positive and negative VM cases are defined by a spring VM index greater than one positive standard deviation and less than one negative standard deviation, respectively. Figure 2c shows that during strong VM years, the CI region experiences anomalously enhanced precipitation exceeding 2 mm d^{-1} at most locations. In contrast, the WI and EI regions experience anomalously reduced precipitation of less than −1 mm d^{-1} at most locations.

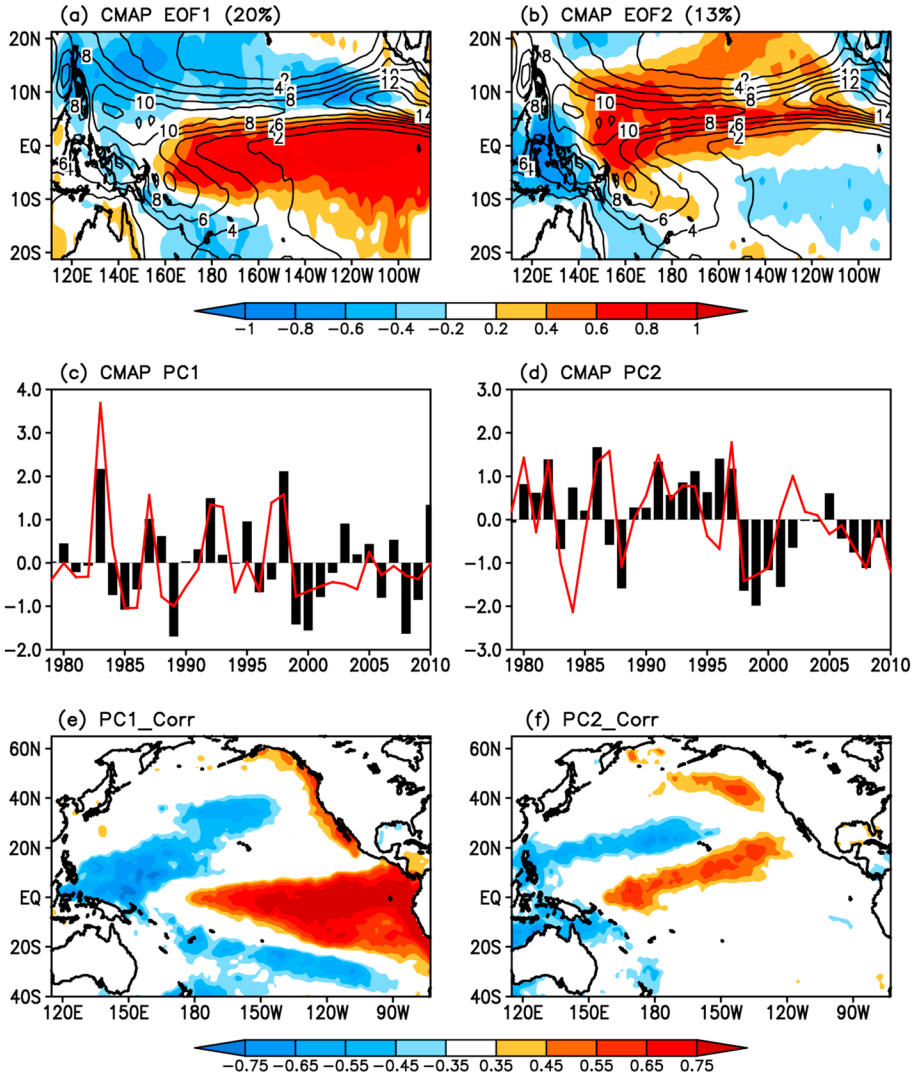

Figure 3. Spatial patterns of the (a) EOF1 and (b) EOF2 modes of the MJJ-averaged normalized precipitation anomalies (mm d^{-1}) in the tropical Pacific (21.25°S–21.25°N, 111.25°E–86.25°W) based on the CMAP data set. Areas with precipitation anomalies greater than 0.2 mm d^{-1} or less than −0.2 mm d^{-1} are shaded. The climatological (1979–2010) summer (MJJ) mean precipitation is superposed as contours. (c) Time series of PC1 (red line) overlaid with the previous winter's (DJF) Niño3.4 index (black bars). (d) Time series of PC2 (red line) overlaid with the previous spring's (FMA) VM index (black bars). (e) Correlation maps of the PC1 time series with the previous winter's Pacific SSTAs. (f) Correlation maps of the PC2 time series with the previous spring's Pacific SSTAs. In Figures 3e and 3f, areas with the correlation coefficients significant at the 95% level are shaded.

Correlations and composites calculated from the GPCP data set (see Figures 2b and 2d) are generally similar to those from the CMAP data set. However, in contrast to the CMAP data, the GPCP data show relatively lower amplitude correlations and composites over the CI region. The correlation between the spring VM index and area-averaged summer GPCP precipitation anomalies over the CI region is 0.44 (significant at the 95% level), which is lower than that (0.59) between the spring VM index and CMAP precipitation anomalies over the CI region. Instead, the GPCP precipitation anomalies show higher correlations with the spring VM index over the region (15°–40°N) to the north of the CI region than over the CI region, which is very different from the CMAP precipitation anomalies. These results are consistent with *Gruber et al.* [2000], who reported that there are significant differences in magnitude and variability between the two data sets in the central-eastern North Pacific (see their Figures 1 and 7).

The above results indicate that the spring VM may significantly affect Pacific ITCZ precipitation during the following summer. It is well known that El Niño–Southern Oscillation (ENSO) is the dominant mode of

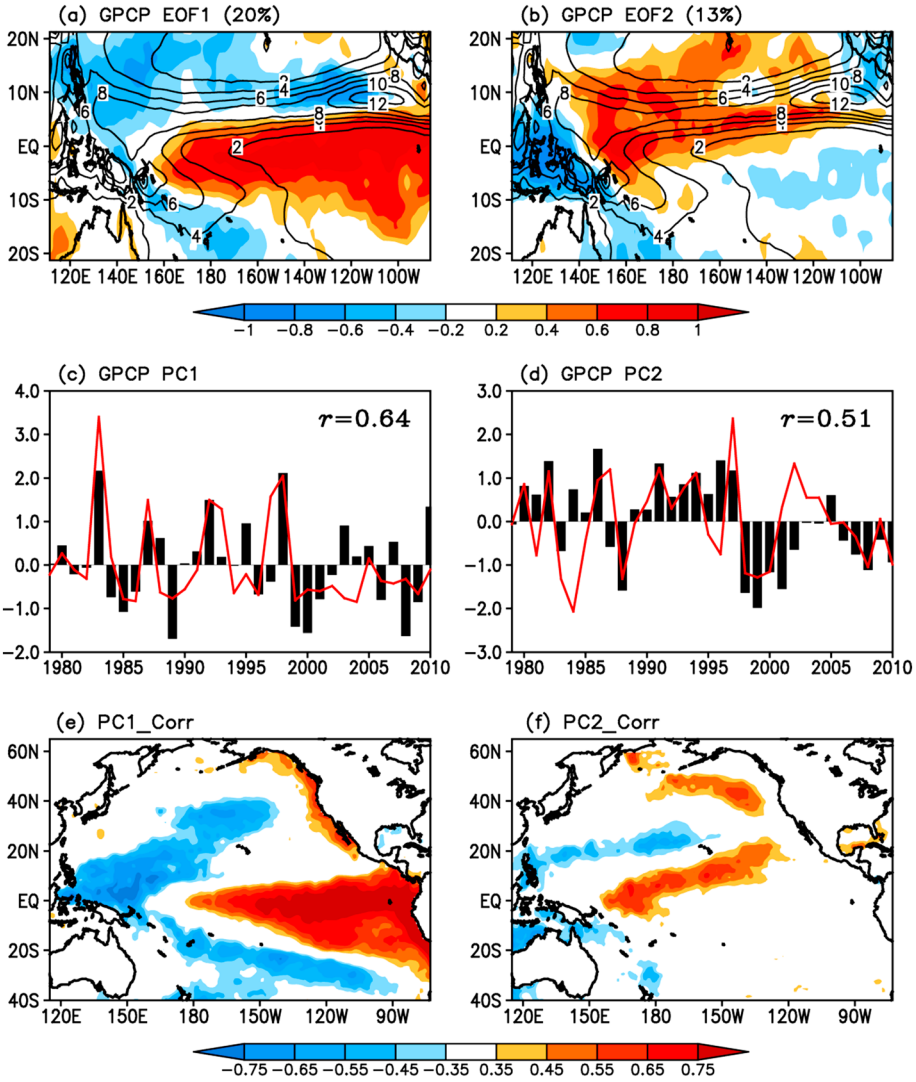

Figure 4. As in Figure 3 but based on the GPCP data set. In Figures 4c and 4d, the correlations between PC1 and the previous winter's (DJF) Niño3.4 index, and between PC2 and the previous spring's (FMA) VM index, are 0.64 and 0.51, respectively.

variability in the tropical Pacific on interannual timescales. Previous studies have confirmed that ENSO has a significant influence on the ITCZ across the whole of the tropics [*Zheng et al.*, 1997; *Hastenrath*, 2002; *Gu et al.*, 2005; *Münnich and Neelin*, 2005; *Chou and Lo*, 2007]. Given that both ENSO and the VM exert a marked influence on the Pacific ITCZ, the question naturally arises as to whether the influences of the VM and ENSO on the Pacific ITCZ are independent. To address this question, we performed EOF analysis on the MJJ-averaged normalized precipitation anomalies for the tropical Pacific (21.25°S–21.25°N, 111.25°E–86.25°W) derived from the CMAP data set. EOF1, which accounts for 20% of the total variance, is characterized by positive precipitation anomalies over the tropical eastern Pacific, extending southward from the southern edge of the ITCZ to near 10°S, and negative precipitation anomalies mainly along the northern edge of the ITCZ (Figure 3a). EOF2, which accounts for 13% of the total variance, closely reproduces the VM composite precipitation anomalies, characterized by positive precipitation anomalies over the CI region, and negative precipitation anomalies over the WI and EI regions (Figure 3b).

The time series for PC1 and PC2 (corresponding to the first two EOFs), overlain by the previous winter (DJF) Niño3.4 and spring (FMA) VM indices, respectively, are shown in Figures 3c and 3d. Table 1 shows that PC1 is significantly correlated with the previous winter's Niño3.4 index ($r = 0.67$, significant at the 99.9% level), while PC2 has a significant correlation with the spring VM index ($r = 0.55$, significant at the 99% level). On the other

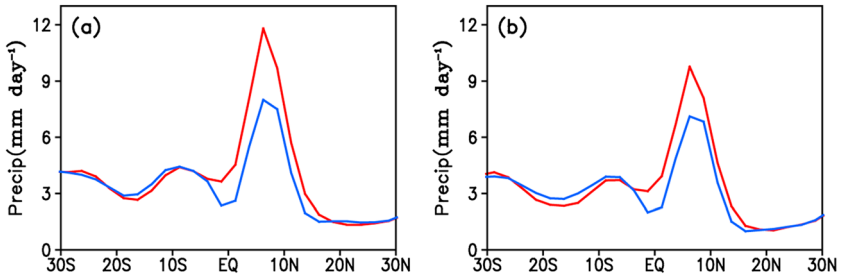

Figure 5. (a) Composite of the zonally averaged summer (MJJ) mean precipitation over 145°E–115°W for strongly positive VM cases (red line) and strongly negative VM cases (blue line) based on the CMAP data set. (b) As for Figure 5a but based on the GPCP data set.

hand, there is only a small correlation between the PC1 and the spring VM index ($r = -0.05$) or between PC2 and the Niño3.4 index from the previous winter ($r = 0.06$). By correlating previous winter Pacific SSTAs with PC1, we find that the spatial pattern of significant correlations robustly shows the typical El Niño pattern in the tropical Pacific (Figure 3e). In contrast, Figure 3f shows that the most significant correlations between PC2 and spring Pacific SSTAs exhibit a tripole structure (including a dipole correlation pattern in the North Pacific poleward of 20°N, along with a subtropical pole of positive correlations located in the central-eastern North Pacific), closely resembling the VM-related SSTA pattern in Figure 1e. Similar EOF patterns and correlation maps were also found based on the GPCP data set (see Figure 4). These consistent results demonstrate that the influences of ENSO and VM on Pacific ITCZ summer precipitation are different and relatively independent. EOF1 is the dominant mode of tropical Pacific summer precipitation anomalies and is closely linked to the previous winter's ENSO, while the EOF2 is the other important mode, which is closely related to the VM from the previous spring.

Previous studies have reported that changes in extratropical forcing may cause distinct southward or northward shifts of the ITCZ [e.g., *Chiang et al.*, 2003; *Zhang and Delworth*, 2005; *Broccoli et al.*, 2006; *Kang et al.*, 2008, 2009]. In contrast, we found that the VM seems to cause a smaller location shift in the precipitation maximum associated with the ITCZ over the central-eastern Pacific (Figures 5a and 5b), mainly because the significant positive precipitation anomalies over the central-eastern North Pacific associated with the VM fall roughly within the bounds of the climatological ITCZ. Therefore, it appears that the VM has a greater influence on the intensity of the Pacific ITCZ than on its position.

In addition, *Di Lorenzo et al.* [2008] reported that the North Pacific Gyre Oscillation (NPGO), defined as the EOF2 of sea surface height anomalies in the central and eastern North Pacific (180°W–110°W, 25°N–62°N), closely tracks the VM. However, although the VM and NPGO are both considered to represent EOF2 of North Pacific climate variability, independent of the PDO [*Mantua et al.*, 1997; *Zhang et al.*, 1997], there are, in fact, remarkable differences between them. *Ding et al.* [2015] show that the NPGO exhibits more prominent low-frequency (decadal) fluctuations than the VM, possibly because of different damping timescales operating on sea surface height (SSH) and SST. They report that on interannual timescales, the VM is more closely linked to the ENSO variability of the tropical Pacific than is the NPGO. We also calculated the correlation between the PC2 and the spring NPGO index (Table 1). They exhibit a correlation of 0.45 (significant at the 99% level), which is lower than the correlation (0.55) between the PC2 and spring VM index, lending support to the idea that the VM is more closely linked to tropical Pacific climate variability on interannual timescales than is the NPGO.

4. Mechanisms

Our results demonstrate that there is a significant relationship between the spring VM and Pacific ITCZ summer precipitation. However, the question of how the spring VM affects the ITCZ during the following summer remains. The mechanisms by which extratropical forcing may influence the ITCZ have been extensively studied [e.g., *Chiang et al.*, 2003; *Chiang and Bitz*, 2005; *Zhang and Delworth*, 2005; *Broccoli et al.*, 2006; *Kang et al.*, 2008, 2009]. However, these previous studies focused on the influences of extratropical forcing on the zonal mean ITCZ location, while few studies have examined in detail how extratropical forcing affects the ITCZ in a local ocean basin (for example, the Pacific ITCZ in this study). In this section, we examine

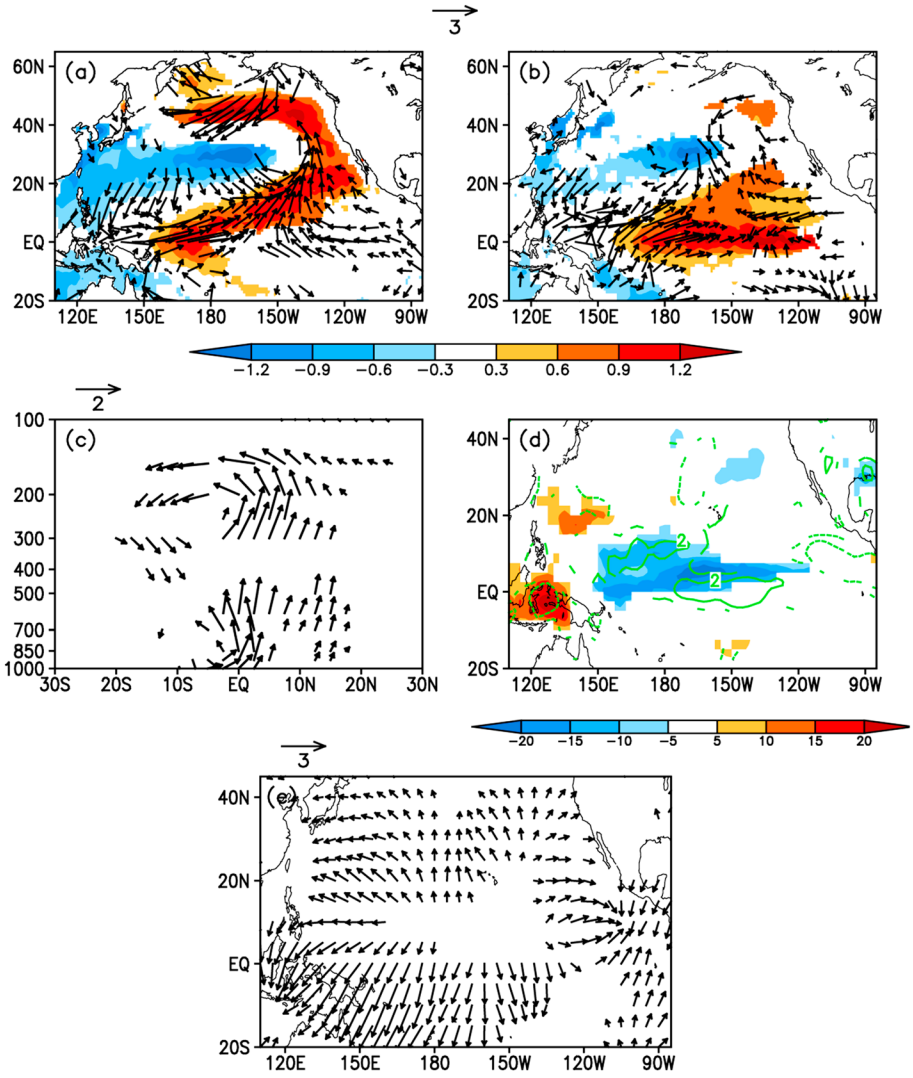

Figure 6. Composite differences in (a) the spring (FMA) and (b) the summer (MJJ) SST (°C; shaded) and surface wind anomalies (m s^{-1}; vectors) between strongly positive and negative VM cases (strongly positive minus negative VM cases). (c) Composite differences in anomalies of the zonally averaged summer meridional (m s^{-1}) and vertical (-10^{-2} pa s^{-1}) components of the velocity for 150°E–105°W between strongly positive and negative VM cases. (d) Composite differences in the 700 hPa summer vertical velocity (-10^{-2} pa s^{-1}; contours) and OLR (W m^{-2}; shaded) anomalies between strongly positive and negative VM cases. (e) Composite differences in the 200 hPa summer divergent wind anomalies between strongly positive and negative VM cases. In Figures 6a–6e, only anomalies significant at the 90% level are shown.

in detail the VM-related SST and atmospheric circulation anomalies, with the aim of identifying the mechanisms connecting the spring VM and Pacific ITCZ summer precipitation.

Figures 6a and 6b show the composite differences in the spring and summer SST and surface wind anomalies between strongly positive and negative VM cases. We can see that the spring VM is associated with a dipole-like SSTA pattern in the North Pacific poleward of 20°N, and a subtropical (0°–20°N) band of positive SSTAs extending from the northeastern Pacific to the tropical central Pacific, consistent with the correlation map in Figure 1e. Surface wind anomalies associated with the VM resemble those associated with the NPO [*Walker and Bliss*, 1932; *Rogers*, 1981], consistent with many previous studies that have suggested that the NPO plays an important role in forcing the anomalous SSTA pattern associated with the VM [*Vimont et al.*, 2003a, 2003b; *Alexander et al.*, 2010; *Yu and Kim*, 2011; *Ding et al.*, 2015]. These significant SST and surface wind anomalies in the North Pacific poleward of 20°N gradually decay over the following summer (Figure 6b). Instead, in response to anomalous southwesterlies associated with the VM during spring

(Figure 6a), the northeasterly trade winds weaken and subsequently reduce the upward latent heat flux (not shown), warming the ocean to the north of the CI region extending from the northeastern Pacific to the subtropical central Pacific and therefore leading to positive wind-evaporation-SST (WES) feedback [*Xie and Philander*, 1994]. This thermodynamic coupling causes spring positive SSTAs in the subtropical central-eastern North Pacific (10°–20°N) to persist until summer (Figure 6b). In contrast to the south of the CI region (0°–10°N), anomalous westerlies in the equatorial western Pacific west of 150°W associated with the VM, combined with anomalous easterlies in the equatorial eastern Pacific east of 150°W, cause convergence and in turn favor the development of positive SSTAs there (Figure 6a). During the ensuing summer, significant positive SSTAs begin to establish to the south of the CI region extending from the subtropical central North Pacific to central equatorial Pacific (Figure 6b). Through these surface air-sea coupling processes associated with the VM, SSTAs in the subtropics associated with the spring VM persist until summer and develop toward the equator.

In addition to significant SST and surface wind anomalies in the tropical Pacific associated with the VM, recent studies have shown that the NPO/VM are also associated with evolution of subsurface ocean temperature anomalies along the equator [*Anderson*, 2004*; Anderson et al.*, 2013; *Ding et al.*, 2015]. They reported that subsurface ocean temperature anomalies along the equator associated with the NPO/VM propagate eastward and upward along the thermocline and reach the surface during summer, finally inducing the warming in the eastern equatorial Pacific (between 150°W and 100°W). Therefore, although anomalous easterlies tend to enhance upwelling and cool the surface in the eastern equatorial Pacific during spring (Figure 6a), there is still marked warming there during the ensuing summer (Figure 6b).

The warming induced by the above processes in the central-eastern tropical Pacific enhances the SSTA gradient across the western South Pacific to central tropical Pacific (also across the eastern to central North Pacific), which then strengthens the anomalous southwesterlies in the western tropical Pacific and forces the anomalous easterlies in the eastern North Pacific (Figure 6b). These winds cause low-level convergence in the central-eastern North Pacific within the latitudes of the ITCZ, leading to vigorous upward motion centered over the CI region (Figure 6d). This enhanced upward motion is superposed on the ascending branch of the local Hadley cell in the tropical central-eastern Pacific, strengthening the latter (Figure 6c) and thereby leading to the enhancement of convection (Figure 6d) and precipitation over the CI region. The enhanced convection and precipitation may result in increased release of the latent heat of condensation into atmosphere, which is favorable for the intensification of the upper level divergence and subsequently low-level convergence, thereby further intensifying the upward motion, convective precipitation, and so on. Finally, this positive feedback process leads to remarkable positive precipitation anomalies over the CI region.

At the same time, anomalous upper level divergent winds generated from enhanced deep convection over the central-eastern North Pacific move southwestward and eastward and then converge over the tropical western Pacific and the eastern North Pacific off the southwest coast of Mexico (Figure 6e), respectively, leading to anomalous downward motion and consequently suppressed convection (Figure 6d) and reduced precipitation over these two ITCZ regions. Note that a weaker anomalous downward motion is seen over the eastern North Pacific, which is consistent with a relatively small precipitation anomaly there. It appears that the ascending motion over the CI region is closely linked to the descending motions over the WI and EI regions, and together, they constitute an anomalous east-west oriented circulation resembling the Walker circulation (but not centered on the equator) across the tropical Pacific. In addition to the large-scale surface convergence or divergence in response to the VM-induced SSTA gradient, local warm or cool SSTAs related to the VM may also increase or decrease convective instability, thereby influencing the local convection and precipitation [*Graham and Barnett*, 1987].

The processes described above suggest that a large-scale surface convergence over the central-eastern North Pacific, which results from the VM-induced SSTA gradient, is an important cause of deep convection and enhanced precipitation over the CI region but suppressed convection and reduced precipitation over the WI and EI regions. Such an atmospheric response to SSTAs in the subtropical Pacific associated with the VM is similar to the tropical atmospheric response to off-equatorial heating reported by *Gill* [1980] and *Lindzen and Nigam* [1987]. In general, the underlying physical process associated with the effects of the spring VM on Pacific ITCZ summer precipitation is similar to but slightly different from the seasonal footprinting mechanism (SFM), proposed by *Vimont et al.* [2001, 2003a, 2003b] to explain the influence of the NPO-like

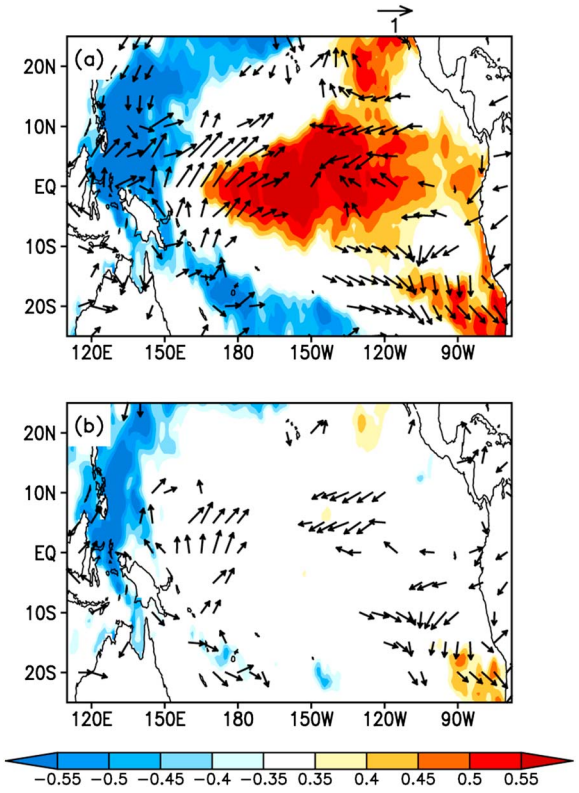

Figure 7. (a) Correlation maps of the spring (FMA) VM index with the following summer's (MJJ) surface winds (vectors) and the following winter's SSTAs (shaded). (b) Partial correlations of the spring VM index with the following summer's surface winds (vectors) and the following winter's (DJF) SSTAs (shaded) by linearly removing the effects of the ITCZ (as represented by the PC2 time series in Figure 3d). In Figures 7a and 7b, the zonal (meridional) component of vectors indicates the correlation between the spring VM index and zonal (meridional) surface winds; areas with correlations significant at the 95% level are shaded, and only surface wind vectors significant at the 95% level are shown.

variability during a particular winter on ENSO during the following winter. The SFM suggested that fluctuations in the wintertime NPO impart an SST footprint onto the ocean via changes in the net surface heat flux. This SST footprint persists until late spring and summer when its subtropical portion (0°–20°N) forces the overlying atmosphere, resulting in zonal wind stress anomalies that favor the initiation of an ENSO event during the following winter. The spring VM SST pattern shown in Figure 6a bears a resemblance to the SST footprint found by *Vimont et al.* [2001, 2003a, 2003b] in both observation and model. Despite the overall similarity between the SST footprint and spring VM SST pattern, however, the emphasis here is on the connection between the VM and Pacific ITCZ precipitation, rather than on the NPO and ENSO. Our analysis indicates that the summer SST and surface wind anomalies in the subtropical Pacific associated with the spring VM are stronger and extend much farther toward the equator than those associated with the spring NPO. As a result, the relationship between the VM and Pacific ITCZ summer precipitation appears to be much more robust than that between the NPO and Pacific ITCZ summer precipitation (not shown). In addition, as mentioned above, the large-scale convergence caused by anomalous surface winds associated with the VM plays an important role in warming the ocean to the south of the CI region extending from the subtropical central North Pacific to central equatorial Pacific, different from the SFM that mainly emphasizes the critical role of the WES feedback in sustaining the NPO-related SSTAs in the subtropics into summer. Actually, our analysis indicates that the WES feedback takes effect mainly in the subtropical central-eastern North Pacific (10°–20°N).

5. Dynamic Links Among the VM, ITCZ, and ENSO

In section 4, we demonstrated that the spring VM exerts a delayed effect on Pacific ITCZ summer precipitation, and this is mainly because SSTAs in the subtropics associated with the spring VM persist until summer and develop toward the equator. *Ding et al.* [2015] reported that the VM may effectively act as an ocean bridge (or conduit) through which the extratropical atmospheric variability in the North Pacific influences ENSO. Since the spring VM can influence both the Pacific ITCZ summer precipitation and ENSO, it is important to ask whether there is any connection between both influences. In this section, we will show that the spring VM influence on Pacific ITCZ summer precipitation is inherently linked to its influence on ENSO.

As shown in Figure 6b, the low-level convergence of surface winds toward the CI region induces anomalous westerlies in the western equatorial Pacific. An increase in low-level convergence over the CI region may lead to increased convective precipitation and latent heat release, which in turn leads to a further increase in low-level convergence, and hence enhanced westerlies in the western equatorial Pacific. This positive feedback may result in the development and persistence of anomalous westerlies in the western equatorial Pacific that are conducive to the initiation of an ENSO event. The PC2 time series in Figure 3d exhibits a high correlation

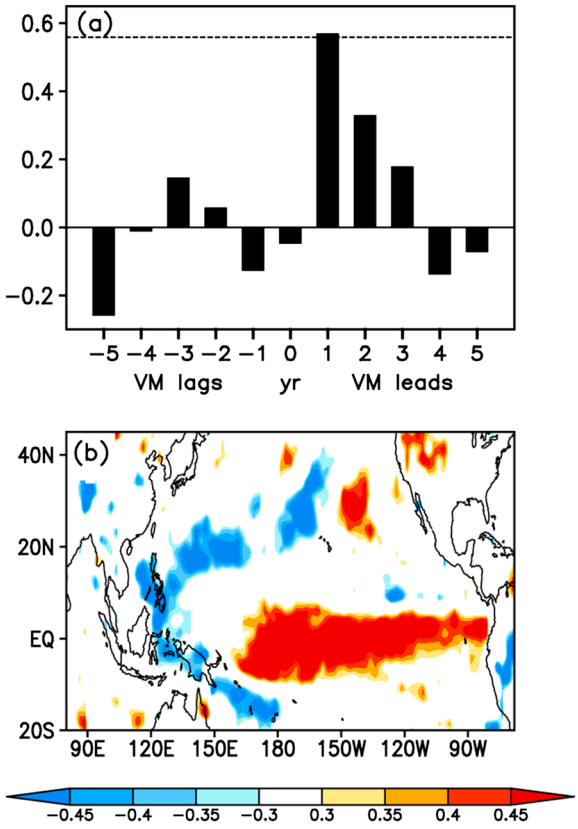

Figure 8. (a) Lead-lag correlations between the spring (FMA) VM index and PC1 time series in Figure 3c. The horizontal dashed line indicates the 99.9% significance level. (b) Correlations of the spring VM index with tropical Pacific summer (MJJ) precipitation of the next year based on the CMAP data set. Areas with correlations significant at the 90% level are shaded.

(0.82, significant at the 99.9% level) with the following winter's (DJF) Niño3.4 index, indicating that changes in the Pacific ITCZ summer precipitation may favor initiation of ENSO events.

To further investigate the importance of Pacific ITCZ summer precipitation in linking the spring VM to ENSO in the following winter, we calculated the partial correlations of the spring VM index with the following summer surface winds and winter SSTAs by linearly removing the effects of the ITCZ (see Figure 7b). With the removal of the ITCZ effect, correlations of anomalous westerlies in the western equatorial Pacific are largely reduced compared with those obtained without the removal of the ITCZ effect (see Figure 7a). Consistent with the reduced correlations of anomalous westerlies along the equator during summer, correlations of SSTAs in the following winter are also largely reduced in most regions of the tropical Pacific, and the El Niño warming pattern almost disappears. These results support the hypothesis that the thermodynamic ocean-atmosphere coupling between the ITCZ and SSTAs associated with the VM in the subtropical Pacific may play a vital role in initiating ENSO events.

Our results are generally consistent with previous studies of the Pacific meridional mode's (PMM) influence on ENSO [*Chiang and Vimont*, 2004; *Chang et al.*, 2007; *Zhang et al.*, 2009a, 2009b]. These studies reported that the PMM is inherent to thermodynamic ocean-atmosphere coupling in ITCZ latitudes and that this thermodynamic coupling plays an important role in sustaining anomalous winds in the deep tropics, forcing equatorially trapped oceanic waves to occur in the central western Pacific, which in turn initiate an ENSO event. The PMM SST pattern is characterized by positive SSTAs in the subtropical central-eastern North Pacific (10°N–30°N) and negative SSTAs in the tropical eastern Pacific [*Chiang and Vimont*, 2004; *Chang et al.*, 2007]. According to Figures 3f and 4f, the spring SSTA pattern followed by anomalous Pacific ITCZ summer precipitation displays a basin-scale SSTA pattern. Its extratropical portion (north of 20°N) bears a resemblance to the VM pattern, while its subtropical/tropical portion resembles the PMM pattern. From Figures 1e and 1f, it is apparent that the VM and PMM patterns are strongly interconnected. The spring VM and PMM SST indices have a high correlation of 0.76 (significant at the 99.9% level) for the period 1979–2010. However, we argue that because the VM is more closely linked to the northern pole of the NPO than the PMM (not shown), the VM may more reflect the role of the extratropical forcing in affecting the Pacific ITCZ summer precipitation, which is exactly the main purpose of this study. Further work is required to examine to what extent the VM → ITCZ → ENSO process can occur independent of variability related to the PMM pattern.

The preceding analysis shows a direct cause-and-effect relationship among the spring VM, tropical Pacific summer precipitation (EOF2), and ENSO in the following winter as follows: VM (spring) → EOF2 (summer) → ENSO (winter). In section 3, we showed that the previous winter's ENSO has an effect on the EOF1 mode of tropical Pacific summer precipitation (Figure 3a). This leads us to speculate that in addition to the direct influence on EOF2, the spring VM can exert a marked influence on the EOF1 mode of tropical Pacific summer precipitation in the following year through its influence on ENSO. Figure 8a shows the lead-lag correlations

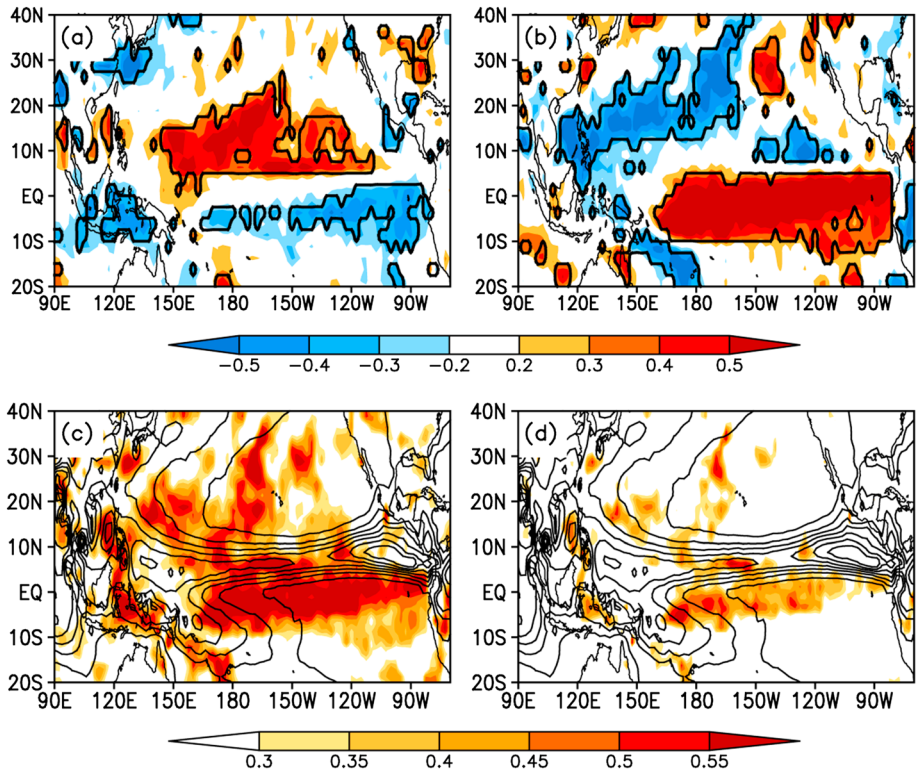

Figure 9. (a) The map of the regression coefficient α (shaded) determined in the empirical prediction model (2). The thick black contours enclose regions with the value of α significantly different from 0 at the 90% level. (b) As for Figure 9a but for the map of the regression coefficient β. (c) Correlations between the observed and hindcast summer (MJJ) precipitation anomalies obtained from the empirical prediction model (2). (d) Correlations between observations and cross-validated hindcasts of summer precipitation anomalies. In Figures 9c and 9d, areas with correlations significant at the 90% level are shaded; the climatological (1979–2010) summer mean precipitation (mm d^{-1}) based on the CMAP data set is superposed as contours.

between the spring VM index and PC1 time series in Figure 3c. We can see that their highest correlation ($r = 0.57$, significant at the 99.9% level) occurs when the spring VM leads the PC1 by 1 year. Correlations between the spring VM index and tropical Pacific summer precipitation of the next year indicate that significant positive correlations occur in the eastern tropical Pacific, while significant negative correlations occur in the western tropical Pacific (Figure 8b), with an anomalous precipitation pattern resembling the EOF1 pattern in Figure 3a. These results support our speculation and suggest that the impact of the VM on tropical Pacific summer precipitation can be passed on to the next year through its influence on ENSO. Therefore, a systematic cause-and-effect relationship among the spring VM, tropical Pacific summer precipitation (including EOF1 and EOF2), and ENSO may exist as follows: VM (spring) → EOF2 (summer) → ENSO (winter) → EOF1 (summer of the next year).

To further examine the contribution of the VM to tropical Pacific summer precipitation, we developed an empirical prediction model for tropical Pacific summer precipitation *P*, at every grid point, using a linear regression method based on both the spring VM index of the current year and the spring VM index of the previous year:

$$P(t) = \alpha \times VM(t) + \beta \times VM(t\text{-}1), \tag{2}$$

where *t* is time in years and the time series of *P*(*t*), *VM*(*t*), and *VM*(*t*-1) have been standardized. The coefficients α and β at one point are obtained by a least-squares fit to the observed *VM*(*t*) and *VM*(*t*-1), respectively. Figures 9a and 9b show the maps of α and β, respectively, with their values significantly different from 0 at the 90% level shaded. We can see that positive values of α significantly different from 0 are mainly located over the CI region, while its significant negative values are mainly located over the WI region and tropical

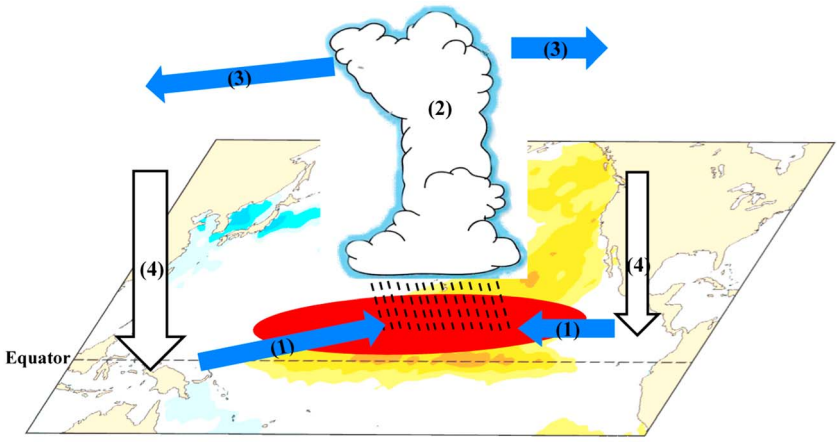

Figure 10. Schematic representation of the thermodynamic ocean-atmosphere coupling between the ITCZ and SSTAs associated with the VM, illustrating how anomalous SST in the subtropical Pacific associated with the VM causes deep convection and enhanced precipitation over the central-eastern Pacific ITCZ region but suppressed convection and reduced precipitation over the ITCZ regions of the tropical western Pacific and eastern North Pacific.

eastern Pacific, with a pattern closely resembling the EOF2 pattern of summer precipitation anomalies in Figure 3b. In contrast, significant positive values of β are mainly located over the tropical central-eastern Pacific, surrounded by significant negative values in the western North Pacific, tropical western Pacific, and western South Pacific, with a pattern closely resembling the EOF1 pattern of summer precipitation anomalies in Figure 3a. These results further suggest that the VM may contribute to both the EOF1 and EOF2 patterns of tropical Pacific summer precipitation anomalies.

Model (2), which uses both the spring VM index of the current year and the spring VM index of the previous year to hindcast the tropical Pacific summer precipitation, yields significant correlations in most regions of the tropical Pacific (Figure 9c). To test the robustness of model (2), the model is cross validated with a leave-one-out procedure (by repeatedly removing 1 year from the period 1979–2010, building a linear regression model based on the spring VM index from the remaining data and hindcasting for the missing year). Correlations between observations and cross-validated hindcasts show some reductions (compared with those in Figure 9c) but still statistically significant in some regions of the tropical Pacific (including the CI and WI regions, and equatorial central-eastern Pacific) (Figure 9d). These results indicate that the VM may be a useful precursor for summer precipitation across almost the entire tropical Pacific. Further research is necessary to examine the real predictive use of the VM precursor as a supplemental tool for the prediction of the tropical Pacific summer precipitation within a forecast framework.

6. Discussion and Conclusions

This study has examined the relationship between the spring VM and the interannual variations in Pacific ITCZ summer precipitation. Our analysis has demonstrated that beyond the well-known influence of ENSO, the VM may significantly impact the interannual variations of Pacific ITCZ summer precipitation. Strongly positive VM cases are followed by positive precipitation anomalies over the CI region, in association with negative precipitation anomalies over the WI and EI regions.

The schematic model in Figure 10 summarizes a possible explanation of processes by which the spring VM affects Pacific ITCZ summer precipitation. During strongly positive VM cases, SSTAs in the subtropics associated with the spring VM persist until summer and develop toward the equator, where low-level convergence and divergence caused by SSTA gradients give rise to vigorous upward motion over the CI

region but anomalous downward motion over the WI and EI regions. The upward motion enhances precipitation over the CI region, while the downward motion reduces precipitation over the WI and EI regions. The suggested physical mechanism through which the spring VM induces Pacific ITCZ summer precipitation anomalies is similar to but slightly different from the SFM that mainly emphasizes the critical role of the WES feedback in sustaining the anomalous SST in the subtropics into summer but considers less the contribution of large-scale convergence of anomalous surface winds to the warming near the equator.

The present analysis suggests that the thermodynamic ocean-atmosphere coupling between the ITCZ and SSTAs in the subtropical Pacific associated with the VM may result in the development and persistence of anomalous westerlies in the western equatorial Pacific and therefore plays a vital role in the initiation of ENSO events. The VM-ITCZ-ENSO dynamic link highlights the potential importance of the VM in contributing to anomalous tropical Pacific summer precipitation. The impact of the VM on tropical Pacific summer precipitation can be passed on to the next year through its influence on ENSO. The important contributions of the VM to anomalous tropical Pacific summer precipitation lead us to speculate that the VM variations may serve as a useful predictor for tropical Pacific summer precipitation. Therefore, we establish an empirical model to predict the tropical Pacific summer precipitation using both the spring VM index of the current year and the spring VM index of the previous year. A cross-validated hindcast performed for the period 1979–2010 yields skillful forecasts for summer precipitation across almost the entire tropical Pacific.

It should be noted that because it is difficult to identify the actual cause-and-effect relationships based on only the correlation and composite analysis of observations, as performed earlier in the present work, further studies (e.g., using state-of-the-art coupled general circulation models) are required to investigate the physical processes associated with the VM, as well as its role in affecting the subsequent Pacific ITCZ summer precipitation and ENSO. In addition, it should be noted that while our results suggest that some ENSO events may be induced by the VM events via the thermodynamic ocean-atmosphere coupling between the ITCZ and VM-related SSTAs, we do not exclude the possibility that other triggering mechanisms, such as the Madden-Julian Oscillation [*Madden and Julian*, 1994] and westerly wind bursts [*McPhaden et al.*, 1992; *McPhaden*, 1999], play an important role for the initiation of these ENSO events. The extent to which the VM affects the occurrence of ENSO via the thermodynamic ocean-atmosphere coupling between the ITCZ and VM-related SSTAs remains unclear; further study is required in this regard.

Furthermore, previous studies have noted that the amplitude of the VM has increased over recent decades [*Bond et al.*, 2003; *Yu et al.*, 2010; *Ding et al.*, 2015]. Consequently, it is likely that the intensified VM has had a greater effect on the Pacific ITCZ during the same period. Prediction of ITCZ precipitation is of great concern to the meteorological community, and we still face many difficulties in predicting the variations in ITCZ precipitation. This study indicates that variations in the VM and ENSO precede the anomalous Pacific ITCZ summer precipitation by 1–2 seasons, suggesting that they may together act as effective predictors of Pacific ITCZ summer precipitation. However, the total variance of the EOF1 and EOF2 modes of the tropical Pacific summer precipitation anomalies, which are closely linked to ENSO and the VM, respectively, is relatively small (<35%). Considering only the roles of ENSO and the VM may be insufficient to understand and predict the variations in ITCZ precipitation. Additional research is required involving a detailed analysis of more EOFs and their physical linkages with local and remote SST forcing. Further analysis of the influence of the VM on the Pacific ITCZ within climate simulation models is also necessary.

Acknowledgments

This research was jointly supported by the 973 project of China (2012CB955200), the National Natural Science Foundation of China (41175069), and the Strategic Priority Research Program of the Chinese Academy of Sciences (XDA11010303). The CMAP and GPCP data sets were obtained from the NASA Goddard Space Flight Center. The atmospheric reanalysis data set was obtained from the NCEP-NCAR. The HadISST data set was obtained from the Met Office Hadley Centre. The OLR data set was obtained from the National Oceanic and Atmospheric Administration (NOAA). The NPGO index is available online at http://www.o3d.org/npgo/data/NPGO.txt. The PMM SST index is available online at http://www.esrl.noaa.gov/psd/data/timeseries/monthly/PMM/.

References

Adler, R. F., et al. (2003), The version-2 Global Precipitation Climatology Project (GPCP) monthly precipitation analysis (1979–present), *J. Hydrometeorol.*, *4*, 1147–1167.

Alexander, M. A., D. J. Vimont, P. Chang, and J. D. Scott (2010), The impact of extratropical atmospheric variability on ENSO: Testing the seasonal footprinting mechanism using coupled model experiments, *J. Clim.*, *23*, 2885–2901.

Anderson, B. T. (2004), Investigation of a large-scale mode of ocean–atmosphere variability and its relation to tropical Pacific sea surface temperature anomalies, *J. Clim.*, *17*, 4089–4098.

Anderson, B. T., R. C. Perez, and A. Karspeck (2013), Triggering of El Niño onset through trade wind–induced charging of the equatorial Pacific, *Geophys. Res. Lett.*, *40*, 1212–1216, doi:10.1002/grl.50200.

Bond, N. A., J. E. Overland, M. Spillane, and P. Stabeno (2003), Recent shifts in the state of the North Pacific, *Geophys. Res. Lett.*, *30*(23), 2183, doi:10.1029/2003GL018597.

Broccoli, A. J., K. A. Dahl, and R. J. Stouffer (2006), Response of the ITCZ to Northern Hemisphere cooling, *Geophys. Res. Lett.*, *33*, L01702, doi:10.1029/2005GL024546.

Chang, P., L. Zhang, R. Saravanan, D. J. Vimont, J. C. H. Chiang, L. Ji, H. Seidel, and M. K. Tippett (2007), Pacific meridional mode and El Niño–Southern Oscillation, *Geophys. Res. Lett.*, *34*, L16608, doi:10.1029/2007GL030302.

Chiang, J. C. H., and C. M. Bitz (2005), Influence of high latitude ice cover on the marine intertropical convergence zone, *Clim. Dyn.*, *25*, 477–496.

Chiang, J. C. H., and D. Vimont (2004), Analogous Pacific and Atlantic meridional modes of tropical atmosphere–ocean variability, *J. Clim.*, *17*, 4143–4158.

Chiang, J. C. H., Y. Kushnir, and A. Giannini (2002), Deconstructing Atlantic intertropical convergence zone variability: Influence of the local cross-equatorial sea surface temperature gradient and remote forcing from the eastern equatorial Pacific, *J. Geophys. Res.*, *107*, 4004, doi:10.1029/2000JD000307.

Chiang, J. C. H., M. Biasutti, and D. S. Battisti (2003), Sensitivity of the Atlantic intertropical convergence zone to Last Glacial Maximum boundary conditions, *Paleoceanography*, *18*(4), 1094, doi:10.1029/2003PA000916.

Chou, C., and M.-H. Lo (2007), Asymmetric responses of tropical precipitation during ENSO, *J. Clim.*, *20*, 3411–3433.

Davey, M. K., et al. (2002), STOIC: A study of coupled model climatology and variability in tropical ocean regions, *Clim. Dyn.*, *18*, 403–420.

Delecluse, P., M. Davey, Y. Kitamura, S. Philander, M. Suarez, and L. Bengtsson (1998), Coupled general circulation modeling of the tropical Pacific, *J. Geophys. Res.*, *103*, 14,357–14,373, doi:10.1029/97JC02546.

Di Lorenzo, E., et al. (2008), North Pacific Gyre Oscillation links ocean climate and ecosystem change, *Geophys. Res. Lett.*, *35*, L08607, doi:10.1029/2007GL032838.

Ding, R. Q., J. P. Li, Y.-H. Tseng, C. Sun, and Y. P. Guo (2015), The Victoria mode in the North Pacific linking extratropical sea level pressure variations to ENSO, *J. Geophys. Res. Atmos.*, *120*, 27–45, doi:10.1002/2014JD022221.

Gill, A. E. (1980), Some simple solutions for heat-induced tropical circulation, *Q. J. R. Meteorol. Soc.*, *106*, 447–462.

Graham, N., and T. P. Barnett (1987), Observations of sea surface temperature and convection over tropical oceans, *Science*, *238*, 657–659.

Gruber, A., X. J. Su, M. Kanamitsu, and J. Schemm (2000), The comparison of two merged rain gauge–satellite precipitation datasets, *Bull. Am. Meteorol. Soc.*, *81*, 2631–2644.

Gu, G. J., R. F. Adler, and A. H. Sobel (2005), The eastern Pacific ITCZ during the boreal spring, *J. Atmos. Sci.*, *62*, 1157–1174.

Hastenrath, S. (2002), The intertropical convergence zone of the eastern Pacific revisited, *Int. J. Climatol.*, *22*, 347–356.

Huffman, G. J., et al. (1997), The Global Precipitation Climatology Project (GPCP) combined precipitation dataset, *Bull. Am. Meteorol. Soc.*, *78*, 5–20.

Kalnay, E., et al. (1996), The NCEP–NCAR 40-year reanalysis project, *Bull. Am. Meteorol. Soc.*, *77*, 437–471.

Kang, S. M., I. M. Held, D. M. W. Frierson, and M. Zhao (2008), The response of the ITCZ to extratropical thermal forcing: Idealized slab-ocean experiments with a GCM, *J. Clim.*, *21*, 3521–3532.

Kang, S. M., D. M. W. Frierson, and I. M. Held (2009), The tropical response to extratropical thermal forcing in an idealized GCM: The importance of radiative feedbacks and convective parameterization, *J. Atmos. Sci.*, *66*, 2812–2827.

Li, X. F., J. J. Yu, and Y. Li (2013), Recent summer rainfall increase and surface cooling over Northern Australia: A response to warming in the tropical Western Pacific, *J. Clim.*, *26*, 7221–7239.

Liebmann, B., and C. A. Smith (1996), Description of a complete (interpolated) outgoing longwave radiation dataset, *Bull. Am. Meteorol. Soc.*, *77*, 1275–1277.

Lin, J.-L. (2007), The double-ITCZ problem in IPCC AR4 coupled GCMs: Ocean–atmosphere feedback analysis, *J. Clim.*, *20*, 4497–4525.

Lindzen, R. S., and S. Nigam (1987), On the role of sea surface temperature gradients in forcing low-level winds and convergence in the Tropics, *J. Atmos. Sci.*, *44*, 2418–2436.

Madden, R. A., and P. R. Julian (1994), Observations of the 40–50-day tropical oscillation—A review, *Mon. Weather Rev.*, *122*, 814−837.

Mantua, N. J., S. R. Hare, Y. Zhang, J. M. Wallace, and R. C. Francis (1997), A Pacific interdecadal climate oscillation with impacts on salmon production, *Bull. Am. Meteorol. Soc.*, *78*, 1069–1079.

McPhaden, M. J. (1999), Genesis and evolution of the 1997–98 El Niño, *Science*, *283*, 950–954.

McPhaden, M. J., F. Bahr, Y. D. Penhoat, E. Firing, S. P. Hayes, P. P. Niiler, P. L. Richardson, and J. M. Toole (1992), The response of the western equatorial Pacific Ocean to westerly wind bursts during November 1989 to January 1990, *J. Geophys. Res.*, *97*, 14,289–14,303, doi:10.1029/92JC01197.

Meehl, G. A., C. Covey, B. McAvaney, M. Latif, and R. J. Stouffer (2005), Overview of the coupled model intercomparison project, *Bull. Am. Meteorol. Soc.*, *86*, 89–93.

Münnich, M., and J. D. Neelin (2005), Seasonal influence of ENSO on the Atlantic ITCZ and equatorial South America, *Geophys. Res. Lett.*, *32*, L21709, doi:10.1029/2005GL023900.

Pyper, B. J., and R. M. Peterman (1998), Comparison of methods to account for autocorrelation in correlation analyses of fish data, *Can. J. Fish. Aquat. Sci.*, *55*, 2127–2140.

Raymond, D. J., G. B. Raga, C. S. Bretherton, J. Molinari, C. López-Carrillo, and Ž. Fuchs (2003), Convective forcing in the intertropical convergence zone of the eastern Pacific, *J. Atmos. Sci.*, *60*, 2064–2082.

Rayner, N. A., P. Brohan, D. E. Parker, C. K. Folland, J. J. Kennedy, M. Vanicek, T. Ansell, and S. F. B. Tett (2006), Improved analyses of changes and uncertainties in sea surface temperature measured in situ since the mid-nineteenth century: The HadSST2 dataset, *J. Clim.*, *19*, 446–469.

Rogers, J. C. (1981), The North Pacific Oscillation, *J. Clim.*, *1*, 39–57.

Vimont, D. J., D. S. Battisti, and A. C. Hirst (2001), Footprinting: A seasonal connection between the tropics and mid-latitudes, *Geophys. Res. Lett.*, *28*, 3923–3926, doi:10.1029/2001GL013435.

Vimont, D. J., J. M. Wallace, and D. S. Battisti (2003a), The seasonal footprinting mechanism in the Pacific: Implications for ENSO, *J. Clim.*, *16*, 2668–2675.

Vimont, D. J., D. S. Battisti, and A. C. Hirst (2003b), The seasonal footprinting mechanism in the CSIRO general circulation models, *J. Clim.*, *16*, 2653–2667.

Walker, G. T., and E. W. Bliss (1932), World weather V, *Mem. R. Meteorol. Soc.*, *4*, 53–84.

Xie, P., and P. A. Arkin (1997), Global precipitation: A 17-year monthly analysis based on gauge observations, satellite estimates, and numerical model outputs, *Bull. Am. Meteorol. Soc.*, *78*, 2539–2558.

Xie, S.-P., and S. G. H. Philander (1994), A coupled ocean–atmosphere model of relevance to the ITCZ in the eastern Pacific, *Tellus*, *46A*, 340–350.

Yin, B., and B. A. Albrecht (2000), Spatial variability of atmospheric boundary layer structure over the eastern equatorial Pacific, *J. Clim.*, *13*, 1574–1592.

Yu, J.-Y., and S. T. Kim (2011), Relationships between extratropical sea level pressure variations and the central Pacific and eastern Pacific types of ENSO, *J. Clim.*, *24*, 708–720.

Yu, J.-Y., H.-Y. Kao, and T. Lee (2010), Subtropics-related interannual sea surface temperature variability in the central equatorial Pacific, *J. Clim.*, *23*, 2869–2884.

Zhan, R. F., Q. Y. Wang, and X.-T. Lei (2011), Contributions of ENSO and East Indian Ocean SSTA to the interannual variability of Northwest Pacific tropical cyclone frequency, *J. Clim.*, *24*, 509–521.

Zhang, L., P. Chang, and L. Ji (2009a), Linking the Pacific meridional mode to ENSO: Coupled model analysis, *J. Clim.*, *22*, 3488–3505.

Zhang, L., P. Chang, and M. K. Tippett (2009b), Linking the Pacific meridional mode to ENSO: Utilization of a noise filter, *J. Clim.*, *22*, 905–922.

Zhang, R., and T. L. Delworth (2005), Simulated tropical response to a substantial weakening of the Atlantic thermohaline circulation, *J. Clim.*, *18*, 1853–1860.

Zhang, Y., J. M. Wallace, and D. S. Battisti (1997), ENSO-like interdecadal variability, *J. Clim.*, *10*, 1004–1020.

Zheng, Q. A., X.-H. Yan, and W. T. Liu (1997), Seasonal and interannual variability of atmospheric convergence zones in the tropical Pacific observed with ERS-1 scatterometer, *Geophys. Res. Lett.*, *24*, 261–263, doi:10.1029/97GL00033.